Conversion-electron Mössbauer study of the interfacial roughness in MBE-grown $Ni_{80}Fe_{20}/Fe_{50}Mn_{50}$ (111) bilayers

R. Jungblut
Philips Research Laboratories, Professor Holstlaan 4, 5656 AA Eindhoven, The Netherlands

Ch. Sauer
Institut für Festkörperforschung, Forschungszentrum Jülich GmbH, 52425 Jülich, Germany

R. Coehoorn, M. T. Johnson, and A. Reinders
Philips Research Laboratories, Professor Holstlaan 4, 5656 AA Eindhoven, The Netherlands
(Received 16 October 1995)

The interface roughness and variations in the magnetic moment at the interface were investigated in epitaxially grown exchange biased $Ni_{80}Fe_{20}/Fe_{50}Mn_{50}$ (111) bilayers by conversion-electron Mössbauer spectroscopy. To this end, a $^{57}Fe_{50}Mn_{50}$ or $Ni_{80}{}^{57}Fe_{20}$ alloy probe layer was inserted at the interface. Using a simple model to analyze the data, it is shown that intermixing at the $Ni_{80}Fe_{20}/Fe_{50}Mn_{50}$ interface is restricted to a zone with a thickness of only two atomic layers. The magnetic moments of Fe atoms in $Ni_{80}Fe_{20}$ close to this zone are not significantly altered.

I. INTRODUCTION

Bilayers of the antiferromagnetic (AF) $Fe_{50}Mn_{50}$ and the ferromagnetic (FM) $Ni_{80}Fe_{20}$ metallic alloys have been studied intensively due to their industrial applications in magnetoresistive sensor materials based on the anisotropic magnetoresistance[1] or on the giant magnetoresistance (''spin-valve'') effect.[2] The exchange coupling at the interface between the AF and the FM layer can cause a unidirectional magnetic anisotropy of the FM layer if the sample is grown in a magnetic field or cooled down in a magnetic field after heating above the blocking temperature of the AF layer. It manifests itself by a shift of the hysteresis loop along the field axis, called the exchange bias field. Tsang, Heiman, and Lee demonstrated that in order to obtain a strong exchange biasing effect it is necessary to have a maximum amount of the metastable fcc-type γ phase of Fe-Mn at the interface.[3] Subsequently, the epitaxial relationship between $Ni_{80}Fe_{20}$ and $Fe_{50}Mn_{50}$ was revealed by Hwang, Geiss, and Howard using cross-sectional TEM studies on sputtered $Ni_{80}Fe_{20}/Fe_{50}Mn_{50}$ bilayers on silicon[4] and by Jungblut *et al.* from low-energy-electron-diffraction (LEED) studies on molecular-beam epitaxy (MBE)-grown $Ni_{80}Fe_{20}/Fe_{50}Mn_{50}$ on [111], [100], and [110]-oriented Cu single-crystal substrates.[5] The latter study and investigations by Rijks *et al.*,[6] where a Ta underlayer was found to improve the degree of [111] texture of the sputter-deposited layers, clearly prove that the [111] orientation leads to the highest biasing effect.

Present theories discuss the exchange biasing phenomenon on the basis of the nearest-neighbor interatomic exchange coupling across the interface, and a specific spin structure in the AF layer, frozen-in during layer fabrication. A brief review of the various models is given in Ref. 5. A crucial aspect in all these models is the crystallographic and magnetic structure near the interface. In the early model by Meiklejohn and Bean[7] the interface structure is assumed to be perfect and the magnetization in the AF layer is assumed to be antiparallel in successive atomic planes parallel to the interface. In the case of ferromagnetic exchange coupling across the interface the preferred direction is given by the frozen-in direction of the magnetization of the interfacial plane of the AF layer. Interfacial roughness, leading to the interaction of the ferromagnetic layer with differently oriented spins in the antiferromagnet would then diminish the exchange biasing effect. On the other hand, in the more recent model by Malozemoff[8] the existence of such an ''uncompensated'' magnetic structure of the outermost atomic layer of the antiferromagnet is not a crucial ingredient. On the contrary, it starts from the assumption of a fully ''compensated'' AF spin structure and discusses the exchange biasing effect as the result of interfacial roughness leading to the formation of domains in the antiferromagnet. For [111]-oriented exchange biased $Ni_{80}Fe_{20}/Fe_{50}Mn_{50}$ Malozemoff's model seems more suitable than the Meiklejohn-Bean model since the in-plane components of the moments within the (111) planes of $Fe_{50}Mn_{50}$ form a fully compensated spin structure.[5]

If interfacial roughness is then a requirement for obtaining the exchange biasing effect in this system it would be very important to establish its actual amplitude and its possible effect on the magnetic moments of the atoms in and near the rough or intermixed interface zone. From earlier ferromagnetic resonance spectra for sputter deposited $Ni_{80}Fe_{20}/Fe_{50}Mn_{50}$ bilayers,[9,10] it was concluded that the magnetization of the permalloy layer near the interface is reduced compared to the bulk value. Stoecklein, Parkin, and Scott[9] found that the ''effective dead layer thickness'' was approximately 5 Å; if tentatively described in terms of a magnetization profile which varies linearly from zero at the nominal interface to the full bulk magnetization at a distance l, then l would be equal to 10 Å. We have attempted to obtain similar information for MBE-grown $Ni_{80}Fe_{20}/Fe_{50}Mn_{50}$ (111) bilayers by

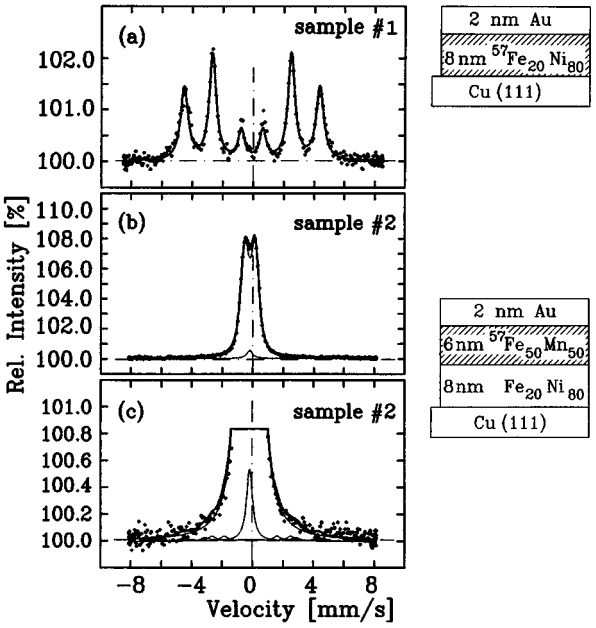

FIG. 1. CEMS spectra at $T=300$ K of (a) the $^{57}Fe_{20}Ni_{80}$ film sample 1 and (b) the $^{57}Fe_{50}Mn_{50}$ film sample 2 for reference. (c) Enlarged scale. The thick solid lines show the best fit.

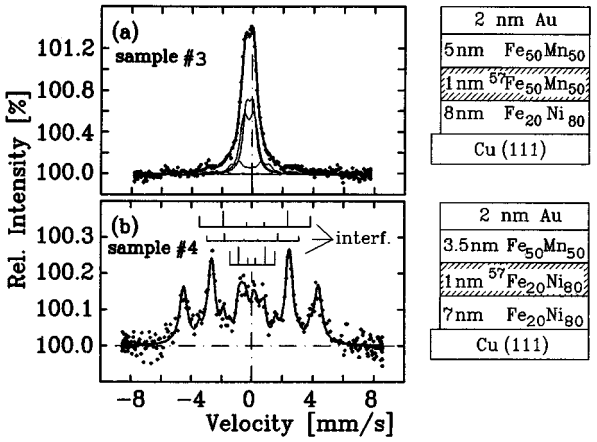

FIG. 2. CEMS spectra at $T=300$ K of samples 3 (a) and sample 4 (b) with a 1 nm thick ^{57}Fe probe layer on the $Ni_{80}Fe_{20}$ and $Fe_{50}Mn_{50}$ side of the interface, respectively. The thick solid lines show the best fits. The thin solid lines and bar patterns are representations of the subspectra into which the data are deconvoluted.

performing a conversion-electron Mössbauer spectroscopy (CEMS) study. Earlier CEMS studies[11] of a series of ^{57}Fe probe atoms inserted at various distances from the interface, have already established the suitability of the technique for obtaining information on interdiffusion and interface roughness on a subnanometer scale. For the $Ni_{80}Fe_{20}/Fe_{50}Mn_{50}$ system with very similar scattering probabilities for the atoms in the two alloys x-ray[12] or neutron reflectometry under grazing incidence[13] are expected to be too insensitive for interface modulations in the monolayer regime. In the present CEMS study, we have inserted either $^{57}Fe_{50}Mn_{50}$ or $Ni_{80}{}^{57}Fe_{20}$ at both sides of the interface. Use is made of the fact that the hyperfine field and electric-field gradient is predominantly determined by the environment of nearest- and next-nearest-neighbor atoms. The samples studied are structurally identical to the MBE-grown $Ni_{80}Fe_{20}/Fe_{50}Mn_{50}$ (111) double-wedge samples for which we reported earlier on the exchange biasing properties.[5] This work supplements these earlier results.

II. EXPERIMENTAL DETAILS

A set of four samples with different ^{57}Fe probe layer positions was evaporated on [111]-oriented Cu single crystals:

sample 1: 8.0 nm Ni_{80} $^{57}Fe_{20}$/2.0 nm Au,
sample 2: 8.0 nm $Ni_{80}Fe_{20}$/6.0 nm $^{57}Fe_{50}Mn_{50}$/2.0 nm Au,
sample 3: 8.0 nm $Ni_{80}Fe_{20}$/1.0 nm $^{57}Fe_{50}Mn_{50}$/5.0 nm $Fe_{50}Mn_{50}$/2.0 nm Au,
sample 4: 7.0 nm $Ni_{80}Fe_{20}$/1.0 nm $^{57}Fe_{20}Ni_{80}$/3.5 nm $Fe_{50}Mn_{50}$/2.0 nm Au.

The structure of the samples is shown in Figs. 1 and 2. The Au layer protects the sample from corrosion. Samples 1 and 2 were made in order to obtain reference spectra for the bulk alloys. In the case of sample 2 the $Fe_{20}Ni_{80}$ layer on the Cu(111) single-crystal substrate served as a buffer for the stabilization of fcc $Fe_{50}Mn_{50}$. Furthermore, all samples investigated had the same total $Ni_{80}Fe_{20}$ thickness in order to avoid possible influences of the microstructure (e.g., stress) of this layer on the $Ni_{80}Fe_{20}/Fe_{50}Mn_{50}$ interface and on the growth of $Fe_{50}Mn_{50}$, as well as to allow a direct comparison of their Mössbauer signals.

Fe and Ni, as well as Fe and Mn were coevaporated from electron-beam evaporators and effusion cells on [111]-oriented Cu single crystals held at room temperature. During the growth a magnetic field of approximately 20 kA/m was applied in plane. Evaporation rates ($Fe_{50}Mn_{50}$ and $Ni_{80}Fe_{20}$:0.08 nm/s) and compositions were controlled by crystal thickness monitors calibrated by chemical analysis. The compositions were controlled by Auger electron spectroscopy with an estimated error of $+/-3$ at. %. The growth quality was characterized by low-energy-electron-diffraction techniques (LEED). The perpendicular and parallel lattice spacings were determined by measuring the energies of the primary Bragg reflections along the [0,0] rod, and by analysis of LEED patterns at constant energy, respectively. When MBE depositing 8 nm $Ni_{80}Fe_{20}$ on the Cu(111) single-crystal substrate, sharp LEED patterns with fcc(111) symmetry and the perpendicular lattice parameter ($d_\perp=0.204\pm0.001$ nm) of the bulk $Ni_{80}Fe_{20}$ were found. Growing $Fe_{50}Mn_{50}$ on Cu(111)/$Ni_{80}Fe_{20}$, only vague (111) LEED patterns were observed for 4.5 nm layer thickness. The perpendicular lattice parameter was found to be relaxed to $d_\perp=0.209\pm0.002$ nm for thicknesses beyond 4.6 nm. A more complete description of the characterization and the growth and magnetic properties of the MBE-grown $Fe_{50}Mn_{50}/Ni_{80}Fe_{20}$ can be found in Ref. 5.

Iron enriched by 95% ^{57}Fe was used for preparing the ^{57}Fe probe layers. It must be mentioned that Fe in its natural composition of isotopes contains 2.17% of ^{57}Fe. This always contributes a small additional Mössbauer signal of ^{57}Fe at-

TABLE I. Fit results of sample 2 ($Fe_{50}Mn_{50}$ reference sample). IS with reference to α-Fe.

Subspectrum	Fits to experimental data B_{hf} [T]	IS (mm/s)	Rel. contribution (%)	Interpretation Assignment
1	27.6±0.2	0.02±0.02	1.1	$Ni_{80}Fe_{20}$ bulk
2	2.99±0.05	−0.09±0.01	94.9	$Fe_{50}Mn_{50}$ bulk
3	18.5±0.3	−0.04±0.03	1.0	Interface
4	0.3±0.3	−0.10±0.02	3.0	Interface

oms which are located outside of the ^{57}Fe probe layer at the position of interest to the Mössbauer spectrum. However, this additional contribution can be calculated from the known film thickness and has been taken into account in our analysis. The CEMS measurements were carried out at room temperature in an UHV chamber with 10^{-9} mbar pressure using a 30 mCi (^{57}Co)Rh Mössbauer source. A channeltron electron detector was mounted in the UHV at a close distance (12 mm) to the thin-film sample for registration of the ^{57}Fe conversion electrons.

III. RESULTS

At first, two samples (1 and 2) were investigated in order to obtain reference Mössbuaer spectra of bulklike $Fe_{50}Mn_{50}$ and $Ni_{80}Fe_{20}$ films. The spectrum of the $^{57}Fe_{20}Ni_{80}$ reference samples (1) is shown in Fig. 1(a). It was fitted by one magnetically split six-line pattern giving a hyperfine field value of $B_{hf}=27.71$ T at room temperature. This value agrees quite well with the result of $B_{hf}=27.6$ T as obtained for a thick $Ni_{81}Fe_{19}$ Permalloy film at 300 K.[14] Due to the random atomic environment of the ^{57}Fe atoms in the alloy film we observed a broadened linewidth of 0.48 mm/s. We remark that the values of the hyperfine fields given here are absolute values. Their sign does not follow from the experiment. For $Ni_{80}Fe_{80}$ it is well known that the actual value is negative.

The Mössbauer spectrum of the $^{57}Fe_{50}Mn_{50}$ reference sample (2) shown in Fig. 1(b), and on an enlarged scale in Fig. 1(c), was fitted by a superposition of four subspectra. The fit parameters are compiled in Table I. The data given on the isomer shift (IS) are with respect to α-Fe. For the conversion of the relative areas of the subspectra into film thicknesses, lattice parameters of 0.204 and 0.209 nm were used for $Ni_{80}Fe_{20}$ and $Fe_{50}Mn_{50}$, respectively.

Subspectrum 1 can be identified by its hyperfine field of $B_{hf}=27.6$ T to belong to the 8 nm thick $Fe_{20}Ni_{80}$ film which should contribute nominally 1.1% to the area of the total spectrum due to the already mentioned natural ^{57}Fe isotope abundance of 2.17%. The observed relative area of 1.1% agrees exactly with this expected contribution. Since bulk $Fe_{50}Mn_{50}$ with an fcc lattice structure is reported[15] to have a hyperfine field at room temperature of $B_{hf}=3.0$ T it is evident that subspectrum 2 corresponds to the $^{57}Fe_{50}Mn_{50}$ film. The measured relative intensity of this spectrum of 94.9% is slightly less than the intensity of 98.9% as expected from the nominal thickness of 6.0 nm $^{57}Fe_{50}Mn_{50}$. Obviously, the missing difference of 4.0% is distributed over the subspectra 3 (1.0%) and 4 (3.0%) which we attribute to ^{57}Fe atoms located directly in the interface zone. Thus the width of this interface zone amounts to approximately 0.24 nm and is, apparently, very small in this sample.

Based on these results of the two reference samples we can now proceed to analyze the Mössbauer spectra of samples 3 and 4 where a 1 nm thick probe layer containing ^{57}Fe was inserted on the $Ni_{80}Fe_{20}$ and $Fe_{50}Mn_{50}$ side of the interface, respectively. The spectrum of sample 3 with the probe layer on the $Fe_{50}Mn_{50}$ side is shown in Fig. 2(a). It was resolved into five subspectra yielding fit parameters as compiled in Table II. Again, subspectra 1 and 2 belong to the $Fe_{20}Ni_{80}$ and $Fe_{50}Mn_{50}$ layers, respectively, according to their hyperfine fields and isomer shifts. But here, subspectrum 2 stems from two regions of the film system: (i) the 5 nm thick $Fe_{50}Mn_{50}$ probe layer. The contribution (ii) corresponding to 1.5 ML thickness shows the correct hyperfine field and isomer shift of bulk $Fe_{50}Mn_{50}$. Based on the values of the hyperfine fields which are between the bulk data of $Fe_{20}Ni_{80}$ and $Fe_{50}Mn_{50}$ we conclude that subspectra 4 and 5 arise from ^{57}Fe atoms located directly at the interface. Their relative contribution amounts to 19.5%, i.e., the interface zone between the $Ni_{80}Fe_{20}$ and $Fe_{50}Mn_{50}$ films is extremely sharp, similarly to the result obtained for the $Fe_{50}Mn_{50}$ reference sample 2. However, there is an additional subspectrum 3 with an hyperfine field of 1.94 T being smaller than the $Fe_{50}Mn_{50}$ bulk field of 2.89 T (Table II). It corresponds

TABLE II. Fit results of sample 3 ($^{57}Fe_{50}Mn_{50}$-probe layer). IS with reference to α-Fe.

Subspectrum	Fits to experimental data B_{hf} (T)	IS (mm/s)	Rel. contribution (%)	Interpretation Assignment
1	27.5±0.2	0.02±0.02	5.2	$Ni_{80}Fe_{20}$ bulk
2	2.89±0.1	−0.11±0.02	38.8	$Fe_{50}Mn_{50}$ bulk
3	1.94±0.1	−0.07±0.02	36.5	2nd, 3rd ML
4	18.3±0.3	−0.02±0.03	5.1	Interface
5	7.8±0.2	−0.02±0.03	14.4	Interface

TABLE III. Fit results of sample 4 ($Ni_{80}{}^{57}Fe_{20}$-probe layer). IS with reference to α-Fe. Subspectrum 3: $\Delta E_Q = -0.1$ mm/s, subspectrum 4: $\Delta E_Q = +0.1$ mm/s; subspectrum 5: $\Delta E_Q = -0.01$ mm/s.

	Fits to experimental data			
Subspectrum	B_{hf} (T)	IS (mm/s)	Rel. contribution (%)	Interpretation Assignment
1	27.60±0.2	0.03±0.02	65.7	$Ni_{80}Fe_{20}$ bulk
2	2.90±0.1	−0.08±0.03	14.0	$Fe_{50}Mn_{50}$ bulk
3	22.60±0.1	0.28±0.04	9.4	Interface
4	19.17±0.5	0.05±0.04	5.0	Interface
5	9.17±0.4	0.06±0.05	5.9	Interface

to a 0.38 nm (1.8 ML) thick zone of the $^{57}Fe_{50}Mn_{50}$ probe layer which will probably be the second and third ML with respect to the interface. We note that a slight change of the hyperfine field at sites in the second and third layer from an interface or surface is well known from band-structure calculations[16] and CEMS investigations.[17,18] The range of those changes extends near interfaces between Fe and other 3*d* metals up to a distance of about 4-5 ML's from the interface.[19] Band-structure calculations for a $Fe_{20}Ni_{80}/Fe_{50}Mn_{50}$ film system would help to clarify this point.

Sample 4 was grown in order to monitor the $Ni_{80}Fe_{20}$ side of the interface. Its Mössbauer spectrum is displayed in Fig. 2(b), and Table III summarizes the results of the deconvolution into five subspectra. Subspectrum 2 is assigned to the $Fe_{50}Mn_{50}$ film containing the natural abundance of 2.17% ^{57}Fe. Its relative intensity of 14.0% corresponds to a film thickness of 3.6 nm in good agreement with the nominal thickness of 3.5 nm. Subspectrum 1 comprises the response of the 7 nm thick $Fe_{20}Ni_{80}$ film containing natural Fe and of a 0.74 nm (3.7 ML) thick part of the 1 nm thick $^{57}Fe_{20}Ni_{80}$ probe layer. As concluded from the intermediate values of the hyperfine fields, subspectra 3–5 are attributed to the $Ni_{80}Fe_{20}/Fe_{50}Mn_{50}$ interface. Their relative contributions add up to 20.3% suggesting a very narrow interface zone with a thickness <2 ML. While for subspectrum 5 almost no quadrupole interaction was observed, the fit yields for subspectra 3 and 4 a quadrupole interaction of $\Delta E_Q = V_{zz}Q/2 = -0.1$ mm/s and $+0.1$ mm/s, respectively. The existence of a quadrupole interaction supports the assignment of these spectra to the interface layer. In order to facilitate a comparison of the different samples the results of the fit and the given interpretations are displayed in Figs. 3(a)–3(c).

IV. ANALYSIS

In order to more quantitatively analyze the results obtained for samples 3 and 4 we make the simplifying assumption that the hyperfine field on Fe varies much less within a certain atomic plane parallel to the interface than in between the neighboring planes. In Fig. 4(a) we show the assumed assignment of the experimental data to the various atomic planes near the interface. There is some uncertainty as regards to assigning the ≈22.6 and ≈19 T subspectra to the same atomic layer, as will be discussed in more detail below. It is thus assumed that the hyperfine field essentially changes within 2 ML which implies that intermixing, if present, occurs on a scale not larger than 2 ML. This profile itself does not exclude that the interface topology is described better by large regions (terraces) with a very sharp compositional separation between the two alloys. We note that Fig. 4 actually gives the absolute values of the hyperfine fields. For Permalloy, the value is certainly negative, but for $Fe_{50}Mn_{50}$ and close to the interface the actual sign is not known.

In order to check the consistency of this assumed profile with the weights of the various subspectra, and in order to obtain extra information about the interfacial intermixing we calculate the composition of the *i*th monolayer. The starting point of the analysis is the profile of hyperfine fields as displayed by Fig. 4(a). We calculated the weights a_i and b_i for the relative $Ni_{80}Fe_{20}$ and $Fe_{50}Mn_{50}$ thicknesses from the weights of the subspectra assigned as ''interface'' in Tables I, II, and III (samples 2, 3, and 4). The condition

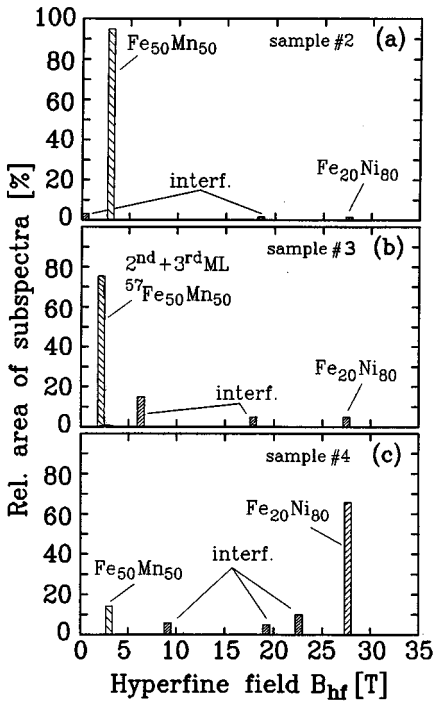

FIG. 3. Hyperfine field distributions as derived from the fits of the CEMS spectra of (a) sample 2 ($^{57}Fe_{50}Mn_{50}$ reference), (b) sample 3 ($^{57}Fe_{50}Mn_{50}$ probe layer) and (c) sample 4 (Ni_{80} $^{57}Fe_{20}$ probe layer).

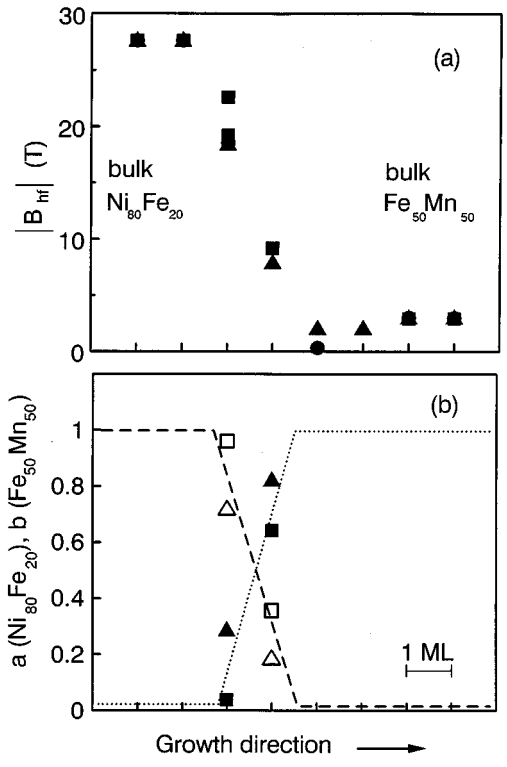

FIG. 4. (a) Hyperfine field distribution as a function of position in the bilayer. B_{hf} compiled from samples 2, 3, 4, (●, ▲, ■); (b) compositional profile in terms of the weights a (-----, open symbols) and b ($\cdots$, solid symbols) of the postulated interface monolayers.

$$a_i(\mathrm{Ni_{80}Fe_{20}}) + b_i(\mathrm{Fe_{50}Mn_{50}}) = 1 \tag{1}$$

must be valid for all layers i. The results are displayed in Fig. 4(b). The weights a, b, describing the interface of sample 3 also give a good description for the concentration profile of sample 2. A subspectrum with $B_{\mathrm{hf}} \approx 8$ T as it was found for samples 3 and 4 is missing in the results of the fits for sample 2. In our model it would contribute to the total area by only $\approx 1\%$ and therefore has no statistical significance. For sample 4, however, the assignment of the subspectrum with $B_{\mathrm{hf}} \approx 22.6$ T to the same atomic layer as the subspectrum with $B_{\mathrm{hf}} \approx 19.2$ T leads to a significantly different set of (a_i, b_i) parameters. As shown in Fig. 4 (squares) this would imply that for sample 4 interfacial mixing was confined to one atomic layer only. However in view of the uncertainty as regards to the assignment of the 22.6 T subspectrum we regard the analysis of sample 3 much more reliable. Our conclusion is thus that intermixing occurs within an interfacial zone with a thickness of two atomic layers.

V. CONCLUSION

We have found that the interface zone in between MBE grown [111]-oriented $\mathrm{Ni_{80}Fe_{20}}$ and $\mathrm{Fe_{50}Mn_{50}}$ layers, in which the hyperfine fields deviate significantly from the bulk values, has a width of only 2 ML. From this we can conclude that even very close to the interface zone the magnetic moments in $\mathrm{Ni_{80}Fe_{20}}$ are not significantly different from their bulk value. From the weights of the subspectra in the samples containing probe layers, it is concluded that nonintegral layer-resolved contributions of probe layer ^{57}Fe atoms to the total occupations of the layer occur across the same thickness range of 2 ML. We believe that this is close to the sharpest possible compositional profile across the interface. This result is expected to provide a clear constraint to future models on the phenomena of exchange biasing.

[1] See, for example, C. Tsang and R. E. Fontana, IEEE Trans. Magn. **MAG-18**, 1149 (1982).
[2] See, for example, B. Dieny, V. S. Speriosu, S. S. P. Parkin, B. A. Gurney, D. R. Wilhoit, and D. Mauri, Phys. Rev. B **43**, 1297 (1991).
[3] C. Tsang, N. Heiman, and K. Lee, J. Appl. Phys. **52**, 2471 (1981).
[4] C. Hwang, R. H. Geiss, and J. K. Howard, J. Appl. Phys. **64**, 6115 (1988).
[5] R. Jungblut, R. Coehoorn, M. T. Johnson, J. aan de Stegge, and A. Reinders, J. Appl. Phys. **75**, 6661 (1994); R. Jungblut, R. Coehoorn, M. T. Johnson, Ch. Sauer, P. J. van der Zaag, A. R. Ball, Th. G. S. M. Rijks, J. aan de Stegge, and A. Reinders, J. Magn. Magn. Mater. **148**, 300 (1995).
[6] Th. G. S. M. Rijks, R. Coehoorn, J. T. F. Daemen, and W. J. M. de Jonge, J. Appl. Phys. **76**, 1092 (1994).
[7] W. H. Meikljohn and C. P. Bean, Phys. Rev. **102**, 1413 (1956); **105**, 904 (1957).
[8] A. P. Malozemoff, Phys. Rev. B **35**, 3679 (1987).
[9] W. Stoecklein, S. S. P. Parkin, and J. C. Scott, Phys. Rev. B **38**, 6847 (1988).
[10] A. Layadi, J. -W. Lee, and J. O. Artman, J. Appl. Phys. **63**, 3808 (1988).
[11] J. Landes, Ch. Sauer, R. A. Brand, W. Zinn, S. Mantl, and Zs. Kajcsos, J. Magn. Magn. Mater. **86**, 71 (1990).
[12] T. C. Huang, J. -P. Nozieres, V. S. Speriosu, H. Lefakis, and B. A. Gurney, Appl. Phys. Lett. **60**, 1573 (1992).
[13] A. R. Ball, H. Fredrikze, P. J. van der Zaag, R. Jungblut, A. Reinders, A. van der Graff, and M. Th. Rekveldt, J. Magn. Magn. Mater. **148**, 46 (1995).
[14] W. Zinn, M. Kalvius, E. Kankeleit, P. Kienle, and W. Wiedemann, J. Phys. Chem. Solids **24**, 993 (1963).
[15] Y. Ishikawa and Y. Endoh, J. Phys. Soc. Jpn. **23**, 205 (1967).
[16] A. J. Freeman, C. L. Fu, M. Weinert, and S. Onishi, Hyperfine Interact. **33**, 53 (1987).
[17] G. Liu and U. Gradmann, J. Magn. Magn. Mater. **118**, 99 (1993).
[18] Ch. Sauer and W. Zinn, in *Magnetic Multilayers*, edited by L. H. Bennett and R. E. Watson (World Scientific, Singapore, 1994).
[19] J. Landes, Ch. Sauer, S. Dörrer, and W. Zinn, J. Magn. Magn. Mater. **113**, 137 (1992).